Cell

The Response of Human Epithelial Cells to TNF Involves an Inducible Autocrine Cascade

Kevin A. Janes,[1,2] Suzanne Gaudet,[1,3] John G. Albeck,[1,3] Ulrik B. Nielsen,[4] Douglas A. Lauffenburger,[1,2,3] and Peter K. Sorger[1,2,3,*]
[1] Center for Cell Decision Processes
[2] Department of Biological Engineering
[3] Department of Biology
Massachusetts Institute of Technology, 77 Massachusetts Avenue, Cambridge, MA 02139, USA
[4] Merrimack Pharmaceuticals, Cambridge, MA 02139, USA
*Contact: psorger@mit.edu
DOI 10.1016/j.cell.2006.01.041

SUMMARY

Tumor necrosis factor (TNF) is a proinflammatory cytokine that induces conflicting pro- and antiapoptotic signals whose relative strengths determine the extent of cell death. TNF receptor (TNFR) has been studied in considerable detail, but it is not known how crosstalk among antagonistic pro- and antiapoptotic signals is achieved. Here we report an experimental and computational analysis of crosstalk between prodeath TNF and prosurvival growth factors in human epithelial cells. By applying classifier-based regression to a cytokine-signaling compendium of ~8000 intracellular protein measurements, we demonstrate that cells respond to TNF both directly, via activated TNF receptor, and indirectly, via the sequential release of transforming growth factor-α (TGF-α), interleukin-1α (IL-1α), and IL-1 receptor antagonist (IL-1ra). We refer to the contingent and time-varying series of extracellular signals induced by TNF as an "autocrine cascade." Time-dependent crosstalk of synergistic and antagonistic autocrine circuits may serve to link cellular responses to the local environment.

INTRODUCTION

Cytokines and their receptors activate complex signaling networks composed of diverse proteins whose overall function is to control cell fate and function (Downward, 2001). Understanding these intracellular networks is complicated in part because many receptors generate competing, and even antagonistic, intracellular signals. For example, tumor necrosis factor (TNF) promotes cell death by inducing activation of the cysteine proteases caspase-8 and caspase-3 (Nicholson and Thornberry, 1997) but also promotes cell survival by activating the nuclear factor-κB (NF-κB) transcription factor (Karin and Ben-Neriah, 2000). In tissues, the connection between signals and cell fate is even more complex because cells are exposed to multiple cytokines that act together in synergistic and antagonistic combinations. Conflicting stimuli often arise when cells are exposed to paracrine cytokines from neighboring cells together with autocrine cytokines secreted by the cell itself. In colonic epithelia, for example, TNF secreted by inflammatory cells is a key mediator of inflammatory bowel disease (Rutgeerts et al., 2004) and can lead to epithelial cell death, whereas locally produced epidermal growth factor (EGF) and insulin-like growth factor (IGF) are critical for cell division and repair of the mucosa (Chailler and Menard, 1999; Singh and Rubin, 1993).

Individual cytokines and receptors have been studied extensively, but relatively little is known about intracellular processing of antagonistic signals. It is likely that crosstalk between individual receptors and their downstream signaling pathways is important. We reasoned that crosstalk could be studied effectively by using a large-scale systematic approach in which cells were treated with antagonistic cytokines and multiple downstream signals were then measured to create a data compendium. We anticipated that most crosstalk would be intracellular and involve the joint regulation of signaling proteins such as mitogen-activated protein kinases, caspases, etc. We therefore assayed intracellular signaling proteins for which reliable quantitative measurements were available (Janes et al., 2003; Nielsen et al., 2003). By focusing on known pathways and proteins, the compendium approach does not seek to identify new signaling proteins but rather to uncover how the activities of known molecules are coordinated during a physiological stimulus. For TNF, our systematic analysis revealed the surprising importance of crosstalk via extracellular autocrine signaling in specifying cell fate.

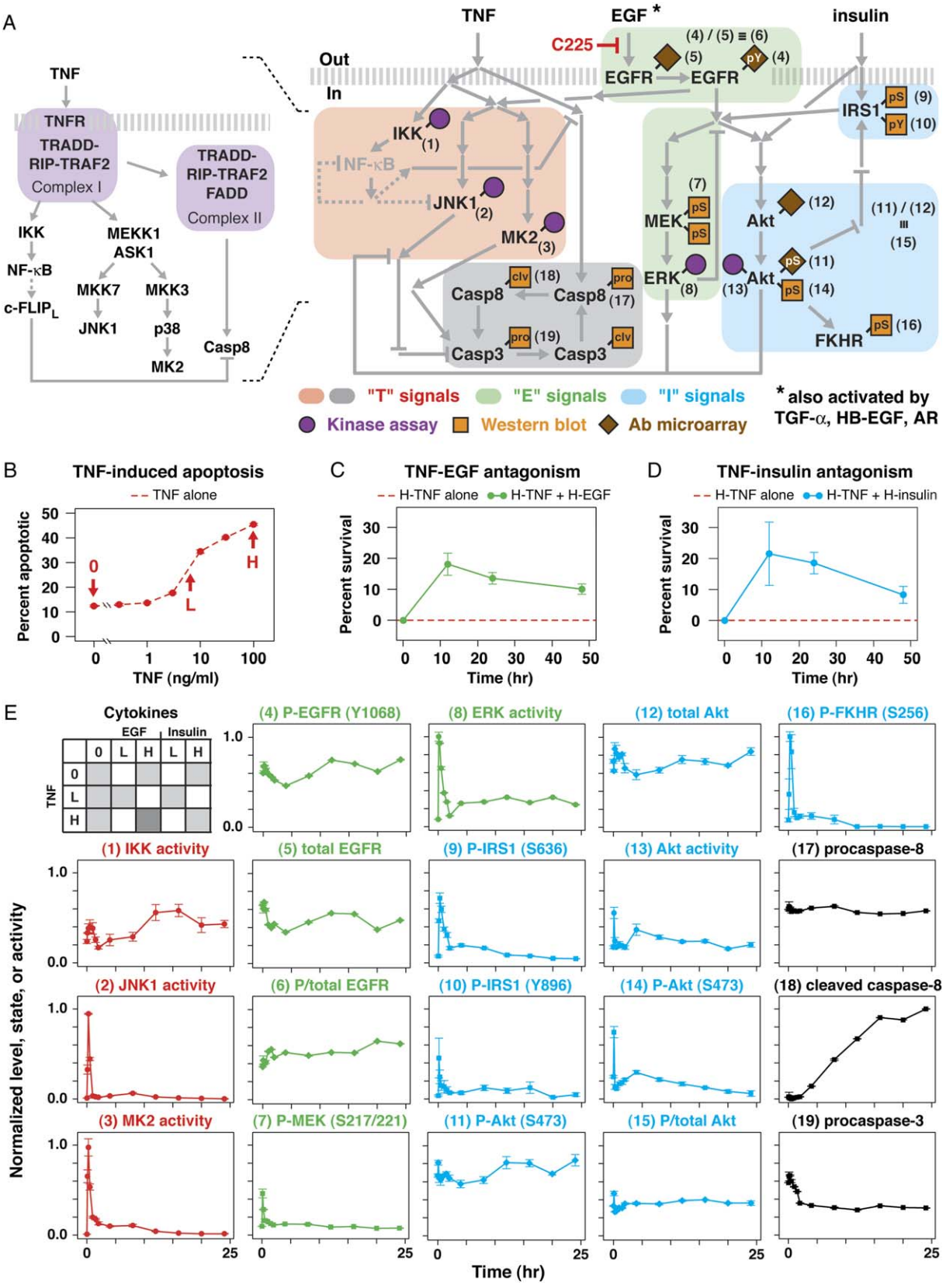
A
TNF
TNFR
TRADD-RIP-TRAF2 Complex I
TRADD-RIP-TRAF2 FADD Complex II
IKK
NF-κB
c-FLIP_L
MEKK1 ASK1
MKK7
MKK3
JNK1
p38
MK2
Casp8
Out
In
EGF *
C225
(4) / (5) ≡ (6)
(5)
(4)
EGFR
EGFR
insulin
IRS1
(9)
(10)
IKK (1)
NF-κB
JNK1 (2)
MK2 (3)
(7)
MEK
ERK (8)
Akt (12)
(11) / (12) ≡ (15)
Akt (13)
(11)
(14)
FKHR (16)
Casp8 (18)
Casp8 (17)
Casp3 (19)
Casp3
"T" signals
"E" signals
"I" signals
Kinase assay
Western blot
Ab microarray
* also activated by TGF-α, HB-EGF, AR
B
TNF-induced apoptosis
TNF alone
Percent apoptotic
TNF (ng/ml)
C
TNF-EGF antagonism
H-TNF alone
H-TNF + H-EGF
Percent survival
Time (hr)
D
TNF-insulin antagonism
H-TNF alone
H-TNF + H-insulin
Percent survival
Time (hr)
E
Cytokines
EGF
Insulin
TNF
Normalized level, state, or activity
(1) IKK activity
(2) JNK1 activity
(3) MK2 activity
(4) P-EGFR (Y1068)
(5) total EGFR
(6) P/total EGFR
(7) P-MEK (S217/221)
(8) ERK activity
(9) P-IRS1 (S636)
(10) P-IRS1 (Y896)
(11) P-Akt (S473)
(12) total Akt
(13) Akt activity
(14) P-Akt (S473)
(15) P/total Akt
(16) P-FKHR (S256)
(17) procaspase-8
(18) cleaved caspase-8
(19) procaspase-3
Time (hr)

TNF is the prototypical member of a family of 19 related proapoptotic and proinflammatory cytokines (Aggarwal, 2003; Chen and Goeddel, 2002). Trimeric TNF binds to a TNF receptor (TNFR) trimer, leading to intracellular assembly of two multicomponent death-inducing signaling complexes, DISC-I and DISC-II (Figure 1A; Barnhart and Peter, 2003; Micheau and Tschopp, 2003). DISC-I is an early membrane bound complex that signals through the NF-κB, JNK, and p38 pathways, whereas DISC-II is a later cytoplasmic complex that activates caspases-8 and -3 (Micheau and Tschopp, 2003). NF-κB signaling from DISC-I antagonizes caspase signaling from DISC-II by inducing transcription of survival factors, such as c-FLIP$_L$, which regulate caspase-8 activation (Micheau et al., 2001, 2002). In many cell types, the proapoptotic functions of TNF are also antagonized by mitogenic cytokines such as EGF, insulin, and IGFs (Garcia-Lloret et al., 1996; Qian et al., 2001; Wu et al., 1996). EGF, insulin, and IGFs bind dimeric receptors that signal via adaptor proteins to ERK, Akt, and other kinase pathways (Figure 1A; Avruch, 1998; Schlessinger, 2004). Growth-factor receptors respond acutely to changes in exogenous ligands and also transduce chronic signals arising from constitutive autocrine stimulation. Autocrine signaling is critically important for the survival and the progression of many cancers (Hambek et al., 2001; Torrance et al., 2000), and small-molecule- and antibody-based therapies have therefore been developed to disrupt receptor-ligand binding, receptor dimerization, and signaling (Hofmann and Garcia-Echeverria, 2005; Mendelsohn and Baselga, 2000). The possibility that these drugs have secondary effects on inflammatory signaling has not been investigated extensively, despite evidence linking inflammation and cancer (Karin and Greten, 2005).

In this paper, we combine conventional and high-throughput experimental methods with numerical analysis to uncover mechanisms of crosstalk involving pro- and antiapoptotic signals induced by TNF. Time-dependent profiles of 19 intracellular signals were measured in cells costimulated with TNF and either EGF or insulin (two prototypical survival factors) to create a cytokine-signaling compendium of ~8000 measurements. We describe elsewhere the experimental methods used to collect, validate, and systematize the compendium (Gaudet et al., 2005) and focus here on the surprising finding that a large fraction of TNF-induced crosstalk occurs extracellularly via regulated shedding of autocrine cytokines. We find that TNF activates a multistep, time-varying "autocrine cascade" in which three secreted factors other than TNF play pro- and antiapoptotic roles: transforming growth factor-α (TGF-α), interleukin-1α (IL-1α), and interleukin-1 receptor antagonist (IL-1ra). Intracellular signaling activated by these cytokines specifies the extent of TNF-induced apoptosis in a self-limiting fashion. While elucidation of the TNF-TGF-α-IL-1α-IL-1ra autocrine cascade involved statistical analysis of a large data compendium, key hypotheses were independently validated using a combination of neutralizing antibodies, small-molecule drugs, and receptor antagonists. We conclude from both large-scale and directed experiments that extracellular autocrine crosstalk plays as important a role as intracellular crosstalk in coordinating cellular responses to TNF.

RESULTS

To explore crosstalk between conflicting mitogenic and apoptotic signals, HT-29 human colonic adenocarcinoma cells were stimulated with TNF in combination with either EGF or insulin. The potency of TNF as a proapoptotic factor in epithelial cells is most apparent when combined with immunostimulatory cytokines such as interferon-γ (IFN-γ; Fransen et al., 1986). Thus, ten combinations of TNF, insulin, and EGF, at either subsaturating ("low" or "L-") or saturating ("high" or "H-") concentrations, were added to HT-29 cells pretreated with IFN-γ for 24 hr (see Experimental Procedures; Figures 1B–1D). A "mock" treatment ("0"), in which cells were manipulated as in other experiments but without added cytokine, served as a baseline control (Figure 1B and data not shown). Triplicate cell extracts were prepared at 13 time points spanning 0 min (before stimulus) to 24 hr, and 19 protein measurements made from each extract. Since many kinase signals

Figure 1. Design and Collection of a TNF-EGF-Insulin Signaling Compendium

(A) Schematic of well-recognized intracellular signaling proteins shared by TNF, EGF, and insulin. Nineteen signals (parentheses) were selected throughout the network and measured by high-throughput kinase assay (Janes et al., 2003), Western blotting, or antibody (Ab) microarray (Nielsen et al., 2003). P/total EGFR (signal 6) and P/total Akt (signal 15) signals were defined by taking the ratio of the phospho- and total signals measured by antibody microarray. Signals were defined as "T" signals (red or black), "E" signals (green), or "I" signals (blue) as described in the text. Dashed arrows indicate transcriptional pathways.

(B) Dose response for HT-29 apoptosis induced by various concentrations of TNF. Apoptosis was measured at 24 hr by annexin V-propidium iodide staining and flow cytometry as described in Experimental Procedures. Mock (0), low (L), and high (H) TNF concentrations were defined at 0, 5, and 100 ng/ml (red).

(C and D) Growth-factor antagonism of TNF-induced apoptosis. HT-29 cells were costimulated with 100 ng/ml TNF (H-TNF) and 100 ng/ml EGF (H-EGF, [C]) or 500 ng/ml insulin (H-insulin, [D]) and compared against 100 ng/ml TNF alone (red) for apoptosis at 12, 24, and 48 hr as described in (B). Percent survival was calculated as described (Janes et al., 2003). Baseline apoptosis values for H-TNF alone were 17%, 36%, and 60% at 12, 24, and 48 hr, respectively.

(E) Signaling network response to 100 ng/ml TNF (H-TNF) and 100 ng/ml EGF (H-EGF). Signals are referenced by number to the targets specified in (A). Data are presented as the mean ± SEM of triplicate biological samples as described in Experimental Procedures. Nine combinations of TNF, EGF, and insulin (shaded boxes, with H-TNF + H-EGF shaded dark gray), as well as a tenth combination of 0.2 ng/ml TNF + 1 ng/ml insulin, were similarly measured and are available in the Supplemental Data.

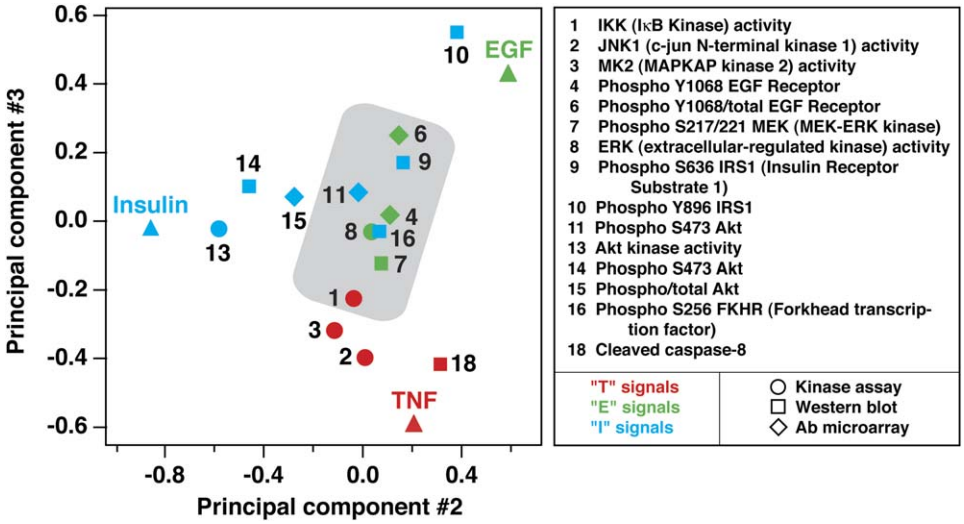

Figure 2. DPLSR Mapping of Intracellular Crosstalk in the Network Shared by TNF, EGF, and Insulin

Data were mapped as described in Experimental Procedures and in Figure S1 (Janes et al., 2004). The numbers, colors, and markers are identical to those in Figure 1E, except for cleaved caspase-8 (signal 18), which has been changed from black to red for clarity. The gray box indicates the crosstalk region shared by TNF, EGF, and insulin.

exhibit rapid changes between 0 and 30 min, whereas caspases rise slowly in activity over many hours, the 13 time points were distributed unevenly, with seven "early" time points concentrated at t = 0–2 hr and six "late" time points spread from t = 4–24 hr. The net result was a multidimensional data set describing time-dependent changes in protein activities following the stimulation of cells with ten distinct cytokine cues.

Considerable effort was expended to ensure the reproducibility and self-consistency of the data (Gaudet et al., 2005). The median coefficient of variation for biological repeats across the full data set was ~11%, making it possible to detect changes in protein state or activity as small as ±15%–25%, even between experiments performed on different days. Inspection of the complete 7980-measurement data set revealed several distinct time courses of signaling. We observed fast-acting "transient" signals, such as c-Jun N-terminal kinase 1 (JNK1) activity, which peaked at 15 min and returned to baseline by 1 hr (Figure 1E, signal 2). Many examples of "sustained" or slow-rising signals were also observed, such as cleaved caspase-8 levels, which began to increase at t > 2 hr and remained high for the duration of the observation period (Figure 1E, signal 18). Based on information in the literature, the 19 measurements acquired at each time point were roughly characterized as TNF-dependent ("T" signals), EGF-dependent ("E" signals), or insulin-dependent ("I" signals; see Figure 1A). Importantly, each cytokine treatment elicited multiple classes of signals: high TNF activated both T and E signals, and high TNF + high EGF elicited T, E, and I signals (Figure 1E and data not shown). We therefore conclude that, as expected, TNF, EGF, and insulin exhibit significant crosstalk at the level of intracellular protein signals.

Mapping Intracellular Crosstalk onto a Shared Cytokine-Signal Space

To visualize connections between intracellular signals and cytokine treatments in a simple and intuitive way, we constructed a compact representation of the entire compendium by using discriminant partial least squares regression (DPLSR; Janes et al., 2004). A DPLSR map was created such that the signaling proteins and cytokines were projected onto a set of "principal components" that maximized covariation between the time-integrated signaling profiles and the corresponding cytokine treatment (see Figure S1 in the Supplemental Data available with this article online for details). The first principal component in the DPLSR map corresponded to a baseline that distinguished all cytokine treatments from mock stimulation, whereas the second and third principal components discriminated among TNF, EGF, and insulin treatments (Figure S1 and data not shown). The latter two principal components therefore identified cytokine-specific signals as well as instances where two or more cytokine pathways had converged upon a common signaling protein.

By plotting cytokine treatments and integrated signals along the two dimensions defined by the second and third principal components, the extent of covariance among signals and treatments could be evaluated. Some cases of covariation were expected: For example, the cleavage of caspase-8 mapped close to TNF (Figure 2, signal 18), consistent with evidence that caspase-8 is activated by TNFR via formation of DISC-II (Micheau and Tschopp, 2003). Similarly, three measures of Akt activity (signals 13–15) mapped close to insulin, which is a powerful inducer of Akt signaling (Avruch, 1998). Sometimes, the map position suggested unexpected biological regulation: For example, the phosphorylation of IRS1 on Y896

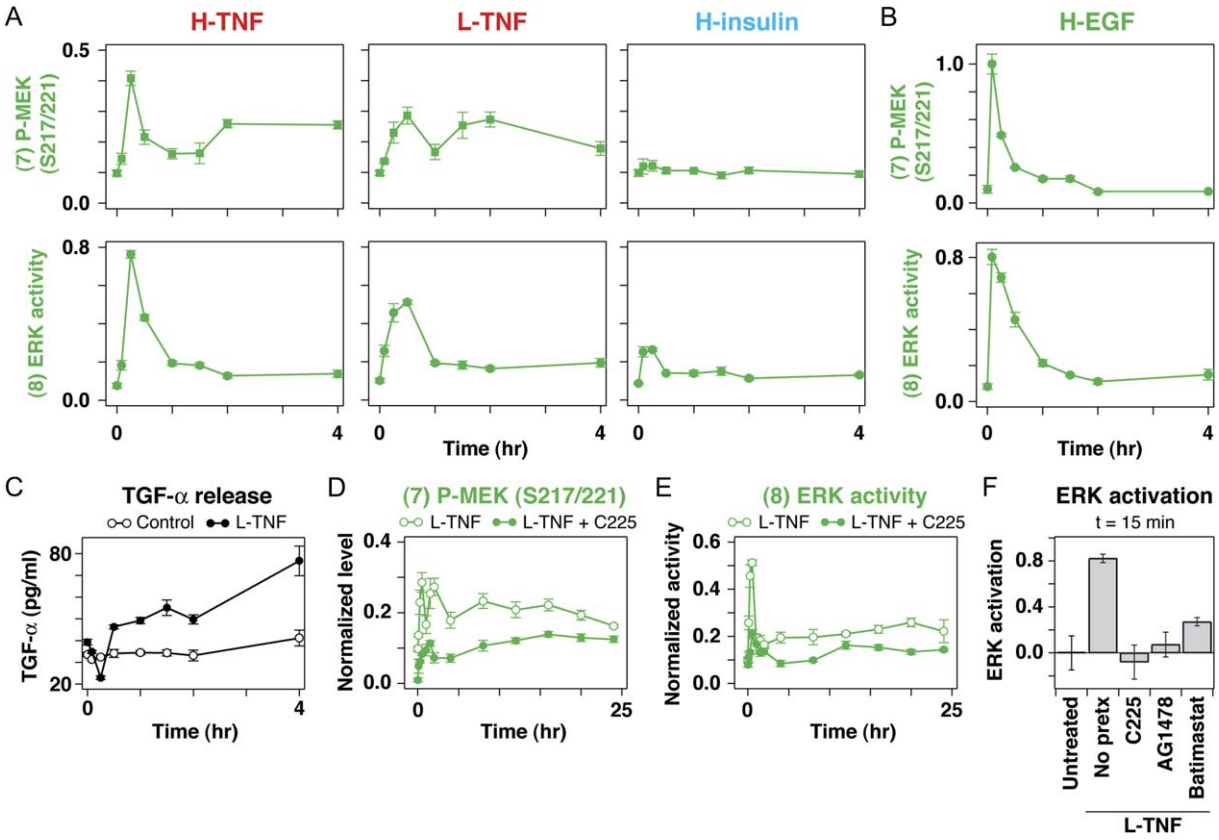

Figure 3. TNF Activates an Early-Phase TGF-α Autocrine Circuit to Crosstalk through the EGFR-MEK-ERK Signaling Pathway

(A) Comparison of P-MEK (upper) and ERK (lower) signaling dynamics induced by 100 ng/ml TNF (H-TNF, left), 5 ng/ml TNF (L-TNF, center), and 500 ng/ml insulin (H-insulin, right). EGFR phosphorylation was similarly increased in response to TNF (data not shown).

(B) Comparison of P-MEK (upper) and ERK (lower) signaling dynamics induced by 100 ng/ml EGF (H-EGF).

(C) TGF-α release in response to 5 ng/ml TNF (L-TNF) in the presence of 10 μg/ml C225 pretreatment for 1 hr before stimulation. The control treatment was a mock stimulation with carrier only. Similar results were obtained in the absence of C225 (data not shown).

(D and E) TNF-induced E signaling through EGFR. pMEK (D) and ERK (E) signaling were measured after stimulation with 5 ng/ml TNF (L-TNF) in the presence or absence of 10 μg/ml C225 pretreatment.

(F) Perturbation of TNF-induced ERK activation by pretreatment with 10 μg/ml C225, 1 μM AG1478, or 10 μM batimastat for 1 hr before stimulation with 5 ng/ml TNF (L-TNF) for 15 min. 0.1% DMSO was added as a control pretreatment (No pretx). ERK activity from untreated cells was included as a baseline, and ERK activation was defined as the increase in ERK activity compared to these untreated cells.

Data are presented as the mean ± SEM of triplicate biological samples as described in Experimental Procedures.

(P-IRS1(Y896); signal 10) was closely associated with EGF but not insulin (Gaudet et al., 2005). Of greatest interest was the clustering of signals midway between TNF, EGF, and insulin, possibly implying covariance of the signals with two or more cytokines (Figure 2, gray box). When the Euclidean distance between cytokine cues and signals in this central cluster was calculated, E signals such as EGFR (Figure 2, signal 4), ERK (signal 8), and MAPK-ERK kinase (MEK, signal 7), were found to be roughly equidistant to TNF and EGF cytokine stimuli but significantly farther from insulin ($p < 0.05$). Inspection of individual cytokine time courses confirmed that TNF treatment activated EGFR, ERK, and MEK to a similar extent as EGF itself, whereas insulin did not (Figures 3A and 3B and data not shown). Others have noted crosstalk between TNF and EGF (Chen et al., 2004; Izumi et al., 1994), supporting the paradoxical conclusion that TNF activates EGFR and its downstream targets MEK and ERK with strength and kinetics similar to EGF.

Rapid Activation of a TGF-α Autocrine Circuit by TNF

A direct intracellular link from activated TNFR to ERK has not been established, but TNF can induce the shedding of EGF-family ligands in mammary epithelial cells following 24 hr of stimulation (Chen et al., 2004). HT-29 cells also shed ligands of the EGF family (Anzano et al., 1989), so we asked whether TNF could stimulate this shedding with the rapid kinetics observed for MEK, ERK, and EGFR activation (Figure 3A and data not shown). EGF-family ligands known to act as autocrine factors include TGF-α, amphiregulin (AR), and heparin binding epidermal growth factor (HB-EGF). Quantitative ELISA measurements of

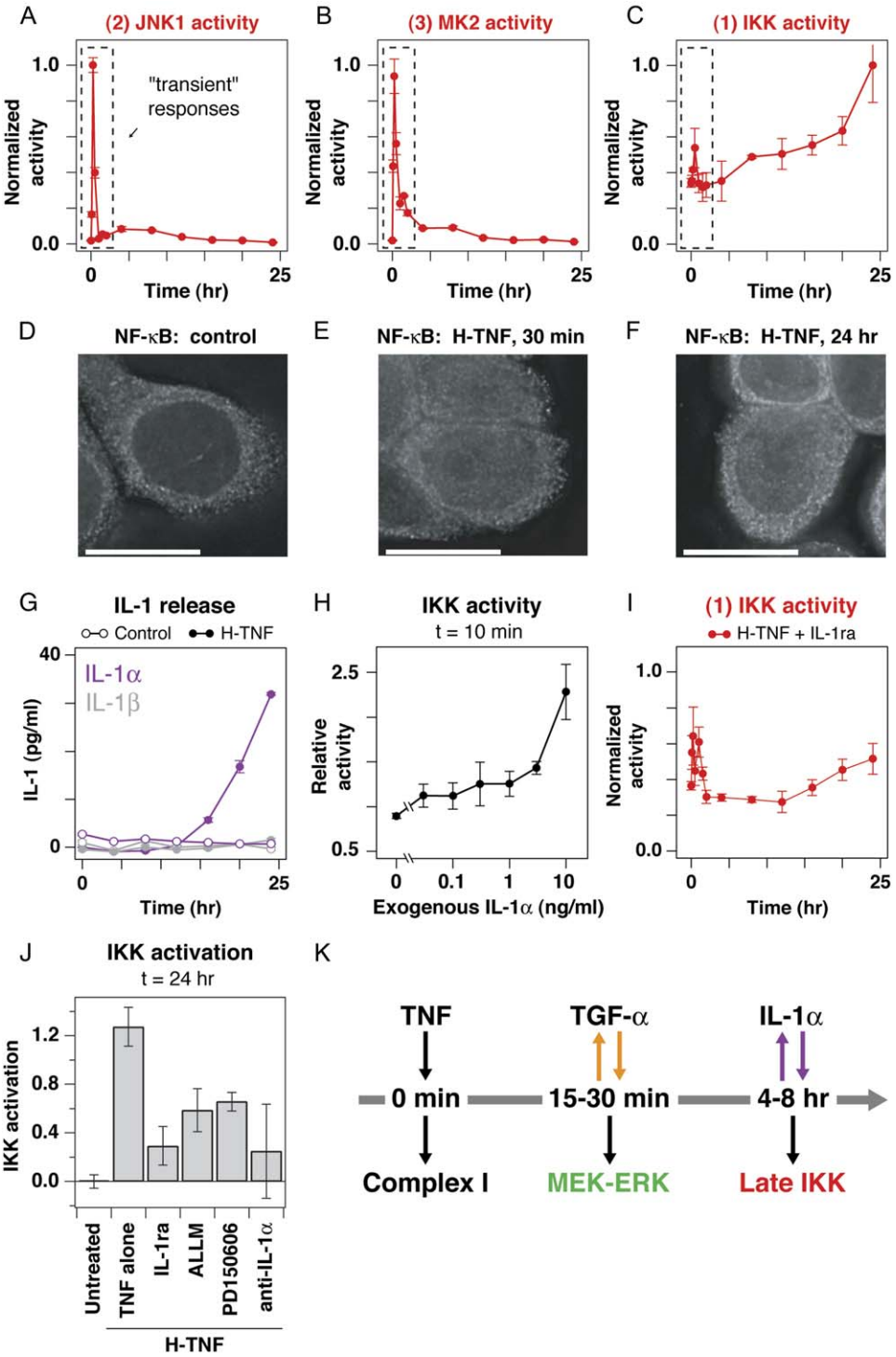

Figure 4. TNF Activates a Late-Phase IL-1α Autocrine Circuit to Crosstalk through the IKK-NF-κB Signaling Pathway

(A–C) TNF-induced signaling after stimulation with 100 ng/ml TNF. JNK1 activity (A), MK2 activity (B), and IKK activity (C) dynamics are shown, with a dotted box highlighting transient responses (t < 2 hr).

(D–F) Indirect immunofluorescence images of the p65 subunit of NF-κB in untreated cells (D) and in cells stimulated with 100 ng/ml TNF (H-TNF) for 30 min (E) and 24 hr (F). Scale bar = 15 μm.

(G) IL-1α (purple) and IL-1β (gray) release in response to 100 ng/ml TNF (H-TNF) in the presence of 10 μg/ml IL-1ra costimulation. The control treatment was a mock stimulation with carrier only. Similar results were obtained in the absence of IL-1ra (data not shown).

EGF-family ligands in conditioned medium of HT-29 cells before and after TNF addition showed all three to be present, but only TGF-α was upregulated by TNF (Figure 3C and Figure S2). TNF-induced TGF-α release in HT-29 cells was much faster than previously reported (Chen et al., 2004), peaking 1 hr after TNF addition (Figure 3C). Thus, TNF stimulation is associated with near-immediate release of an EGFR ligand, TGF-α, into the medium. Although transcriptional upregulation of TGF-α by growth-factor signaling pathways has been reported (Schulze et al., 2001), the rapidity of TGF-α release after TNF treatment suggests a posttranslational mechanism.

Addition of exogenous EGF rapidly activated MEK and ERK in HT-29 cells (Figure 3B). We therefore asked whether TNF-stimulated release of endogenous TGF-α also activated MEK and ERK in an EGFR-dependent fashion. When cells were treated with C225 antibody to block the interaction of EGFR with its ligands (Figure S3), dramatic inhibition of both acute (t = 0–2 hr) and sustained (t = 2–24 hr) MEK-ERK activation was observed after TNF treatment (Figures 3D and 3E). The significant and persistent reduction in MEK-ERK signaling following TNF stimulation (4-fold lower at t = 30 min, $p < 0.005$ and 2-fold lower at t = 4–24 hr, $p < 10^{-6}$) demonstrates a predominantly EGFR-dependent pathway. ERK activation was also blocked by a small-molecule inhibitor of the EGFR kinase (AG1478) and an inhibitor of the matrix metalloproteases that mediate TGF-α shedding from the plasma membrane (batimastat; Peschon et al., 1998; Figure 3F). Taken together, these data show that an autocrine circuit involving TGF-α and EGFR is the primary mechanism by which TNF activates MEK-ERK signaling at both short (t < 1 hr) and long (t > 4 hr) timescales in HT-29 cells. The delay between the peak of direct ERK activation by EGF at t = 5 min and indirect activation by TNF at t = 15 min is an estimate of the minimum time required to establish the TNF-induced TGF-α autocrine circuit (Figure 3A).

TNF Activates a Late-Phase IL-1α Autocrine Circuit

Further inspection of the DPLSR map revealed that IKK activity (Figure 2, signal 1) was also unexpectedly distant from its presumed inducer, TNF. JNK1 and MK2 are two well-recognized TNF-induced signals that, unlike IKK, were close to TNF on the DPLSR map (Figure 2, signals 2 and 3; Wajant et al., 2003). We therefore compared the dynamics of their activation to that of IKK. All three T signals were strongly induced 5–30 min after TNF addition, but IKK was unique in exhibiting a second, sustained phase of activation, rising from 4–24 hr (Figures 4A–4C). In the classical TNF-induced pathway, IKK phosphorylates and inactivates IκB, an NF-κB inhibitor, which allows NF-κB to translocate into the nucleus and induce gene expression (Karin and Ben-Neriah, 2000). By immunofluorescence, we found that the p65 subunit of NF-κB—which was largely cytoplasmic before TNF stimulation, reflecting its sequestration by IκB (Figure 4D)—was present at high levels in the nucleus in TNF-treated cells during early (t = 30 min) and late (t = 24 hr) peaks of IKK activation (Figures 4E and 4F). Thus, the two distinct phases of IKK signaling both appear to activate NF-κB. However, since JNK1 and MK2 activities had returned to low levels by t = 1 hr (Figures 4A and 4B), it seemed unlikely that sustained IKK and NF-κB signaling at t > 4 hr was mediated directly by TNF.

One circumstance in which sustained NF-κB activation is well described is in ultraviolet-irradiated keratinocytes, where late NF-κB signaling is known to depend on secondary release of IL-1α (Bender et al., 1998). Because IL-1 cytokines are potent IKK agonists (Dinarello, 1997), we asked whether TNF treatment of HT-29 cells might lead to IL-1 release and whether IL-1 would provoke sustained IKK activation. We observed an 8-fold increase in soluble IL-1α, but not IL-1β, in conditioned medium from TNF-treated cells 12–24 hr after TNF addition (Figure 4G). HT-29 cells are known to express the IL-1 receptor (IL-1R; Panja et al., 1998), and we found that exogenous IL-1α activated IKK at concentrations as low as 30 pg/ml (Figure 4H), consistent with the recognized ligand sensitivity of IL-1R (Dinarello, 1997). Thus, HT-29 cells are IL-1 responsive and secrete IL-1α after TNF stimulation, suggesting that IL-1α might constitute a TNF-dependent activator of IKK.

To determine whether IKK activation in TNF-treated cells was dependent on secreted IL-1α, IKK activity was measured in cells treated with high TNF in the presence of saturating levels of IL-1ra, a naturally occurring IL-1R antagonist (Figure S3; Dinarello, 2000). We observed that activation of IKK 15–30 min after TNF addition was unaltered by IL-1ra, consistent with a direct pathway via TNFR (Figure 4I). However, sustained IKK activation 4–24 hr after TNF addition was significantly reduced by IL-1ra addition ($p < 0.001$; Figures 4C and 4I). Substantial reductions in TNF-induced IKK activity at 24 hr were also observed with ALLM and PD150606, two structurally distinct calpain inhibitors that block processing and release

(H) IKK activity induced by recombinant IL-1α. HT-29 cells were stimulated with various concentrations of exogenous IL-1α for 10 min and analyzed for IKK activity.

(I) IKK response to 100 ng/ml TNF (H-TNF) with 10 μg/ml IL-1ra cotreatment. Cells were treated and measured for IKK activity as shown in (C) but in the presence of IL-1ra.

(J) Perturbation of TNF-induced IKK activation by cotreatment with 10 μg/ml IL-1ra, 25 μM ALLM, 25 μM PD150606, or 1 μg/ml anti-IL-1α during stimulation with 100 ng/ml TNF (H-TNF) for 24 hr. IKK activity from untreated cells was included as a baseline, and IKK activation was defined as the increase in IKK activity compared to these untreated cells.

(K) Timeline of TNF-induced TGF-α and IL-1α autocrine circuits and autocrine-dependent signals.

For (A)–(C) and (G)–(J), data are presented as the mean ± SEM of triplicate biological samples as described in Experimental Procedures.

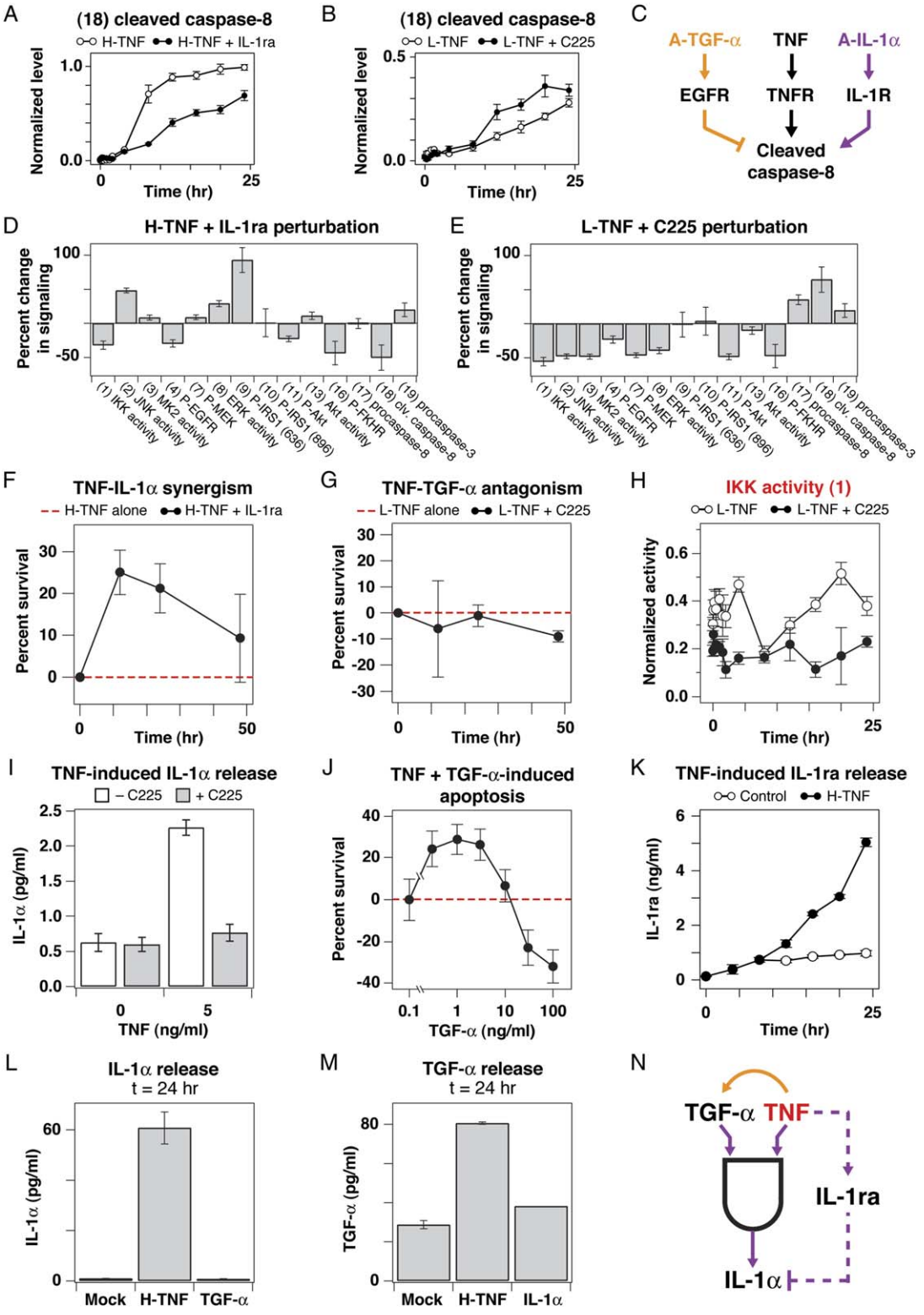

Figure 5. The TNF-Induced TGF-α and IL-1α Circuits Are Coupled with an IL-1ra Circuit to Form an Autocrine Cascade

(A and B) Quantitative changes in TNF-induced caspase signaling after perturbation of the TGF-α and IL-1α autocrine circuits. Cleaved caspase-8 responses to 5 ng/ml TNF (L-TNF) with or without 10 μg/ml C225 pretreatment (A) or 100 ng/ml TNF (H-TNF) with or without 10 μg/ml IL-1ra cotreatment (B). TNF-induced procaspase-3 signaling was also affected by IL-1ra (data not shown).

of IL-1α from cells (Kobayashi et al., 1990), as well as with IL-1α-neutralizing antibodies (Figure 4J). Together, these data show that IKK signaling at t < 4 hr is independent of IL-1α but that sustained IKK activation at t > 4 hr (which is quantitatively more significant in HT-29 cells; Figure 4C) is mediated primarily by the binding of IL-1α to IL-1R (Figure 4K). Thus, the early and late phases of IKK activation in TNF-treated HT-29 cells involve distinct direct and autocrine-indirect mechanisms.

Coupling of Sequential Autocrine Circuits into an Autocrine Cascade

The data described above establish that TGF-α and IL-1α autocrine circuits play important roles in the activation of MEK-ERK and IKK by TNF, but it remained unclear whether autocrine-dependent signaling altered the activity of caspases directly implicated in apoptosis. To study this, we blocked TGF-α- and IL-1α-dependent circuits individually and measured the cleavage of caspase-8, an important initiator caspase downstream of TNFR (Chen and Goeddel, 2002). Blocking IL-1R with IL-1ra significantly reduced TNF-stimulated cleavage of caspase-8 compared to TNF alone ($p < 10^{-9}$; Figure 5A). Conversely, blocking EGFR with C225 significantly increased TNF-induced caspase-8 cleavage ($p < 0.001$; Figure 5B). Thus, TNF-induced TGF-α and IL-1α exert opposing control on caspase-8 (Figure 5C). To determine how broad an effect EGFR or IL-1R blockade had on TNF-induced signaling, full time courses were collected for the 19 signals after TNF stimulation in the presence of IL-1ra or C225. When autocrine-perturbed time courses were compared to data in the original cytokine-signaling compendium, we found that the durations or magnitudes of roughly half of the measured signals were altered (Figures 5D and 5E). Thus, discrete perturbation of an autocrine circuit causes a system-wide alteration in the underlying intracellular signaling network.

The opposing contributions of TGF-α and IL-1α to TNF-induced caspase-8 cleavage implied that blocking EGFR-mediated signaling should decrease cell survival, whereas blocking IL-1R-mediated signaling should decrease cell death (Figure 5C). Consistent with this, we observed that TNF was less effective as a prodeath stimulus when IL-1α signaling was blocked with IL-1ra (Figure 5F). The potency of IL-1ra as a prosurvival factor in TNF-treated cells was comparable to that of saturating EGF or insulin (Figures 1C and 1D). In contrast, blocking TGF-α signaling with C225 antibody did not substantially increase TNF-induced cell death (Figure 5G). This was paradoxical because it implied that the ability of autocrine TGF-α to reduce caspase-8 cleavage (Figure 5C) did not translate into reduced cell death. In an attempt to resolve this paradox, the 19 signals measured for TNF + C225 treatment were examined more closely (Figure 5E). We observed that IKK activity was reduced to baseline levels throughout the time course, exhibiting neither early- nor late-phase activation ($p < 10^{-10}$; Figure 5H). The attenuation of late-phase IKK signaling (t = 4–24 hr) by C225 was particularly interesting because our results indicated that late-phase IKK signaling required an autocrine IL-1α circuit (Figures 4C and 4I). Therefore, it seemed possible that induction of the IL-1α circuit (and thus late IKK signaling) might depend upon prior release of TGF-α. To determine whether TGF-α and IL-1α release were linked, we blocked TGF-α-EGFR signaling with C225 and measured IL-1α levels following TNF stimulation. EGFR blockade with C225 completely prevented IL-1α release at low TNF concentrations (Figure 5I) and significantly reduced IL-1α release at high

(C) Autocrine TGF-α (A-TGF-α) and autocrine IL-1α (A-IL-1α) exert opposing control on TNF-induced caspase-8 cleavage.
(D and E) Network-level changes in TNF-induced signaling in the presence of 10 μg/ml C225 pretreatment (D) or 10 μg/ml IL-1ra cotreatment. Selected intracellular signals from C225- and IL-1ra-treated cells were integrated from 0–24 hr and compared to the integrated signals from 5 ng/ml TNF (L-TNF) and 100 ng/ml TNF (H-TNF) treatments without autocrine perturbation, respectively. Uncertainty in the integrated signaling profiles was calculated by bootstrapping with the original signaling replicates (Efron and Tibshirani, 1993).
(F) IL-1α-mediated synergism with TNF-induced apoptosis. HT-29 cells were cotreated with 100 ng/ml TNF (H-TNF) and 10 μg/ml IL-1ra and compared against H-TNF alone (red) for apoptosis at 12, 24, and 48 hr as described in Figure 1B (Janes et al., 2005). Baseline apoptosis values for H-TNF alone were 17%, 45%, and 67% at 12, 24, and 48 hr, respectively.
(G) TGF-α-mediated antagonism of TNF-induced apoptosis. HT-29 cells were pretreated with 10 μg/ml C225, stimulated with 5 ng/ml TNF (L-TNF), and compared against L-TNF alone (red) for apoptosis at 12, 24, and 48 hr as described in Figure 1B (Janes et al., 2005). Baseline apoptosis values for L-TNF alone were 11%, 24%, and 47% at 12, 24, and 48 hr, respectively.
(H) IKK response to 5 ng/ml TNF (L-TNF) with or without 10 μg/ml C225 pretreatment.
(I) IL-1α release induced by 0 or 5 ng/ml TNF with or without 10 μg/ml C225 pretreatment. The control treatment was a mock stimulation with carrier only.
(J) TGF-α-mediated antagonism for TNF-induced apoptosis. HT-29 cells were treated with various concentrations of TGF-α and 5 ng/ml TNF (L-TNF) and compared against L-TNF alone (red) for apoptosis at 24 hr as described in Figure 1B (Janes et al., 2005). Baseline apoptosis for L-TNF alone was 33%.
(K) IL-1ra release in response to 100 ng/ml TNF (H-TNF). The control treatment was a mock stimulation with carrier only.
(L) The IL-1α autocrine circuit is induced by TNF but not by TGF-α. HT-29 cells were treated with 100 ng/ml TNF (H-TNF) or 100 ng/ml TGF-α for 24 hr and analyzed for IL-1α release.
(M) The TGF-α autocrine circuit is induced by TNF but not by IL-1α. HT-29 cells were treated with 100 ng/ml TNF (H-TNF) or 10 ng/ml IL-1α for 24 hr and analyzed for TGF-α release.
(N) The molecular logic of the TNF-induced autocrine cascade. TNF, TGF-α, and IL-1α are coupled via an "AND" gate.
For (A)–(B) and (F)–(M), data are presented as the mean ± SEM of triplicate biological samples as described in Experimental Procedures. For (D) and (E), data are presented as the mean percent change ± SD from 1000 resamplings of the original data set.

TNF concentrations (Figure S4). Thus, proper function of the IL-1α autocrine circuit was dependent on the prior establishment of an EGFR-mediated TGF-α circuit.

The observed coupling between TGF-α and IL-1α autocrine circuits explains the inability of EGFR blockade to alter TNF-induced cell death significantly. In TNF-treated cells, C225 increased cleaved caspase-8 levels and reduced MEK-ERK signaling (which is generally regarded as a prosurvival signal; Ballif and Blenis, 2001), but C225 also prevented IL-1α release (Figure 5I), which mediates proapoptotic signals via IL-1R (Figure 5F). The ability of C225 to block the offsetting TGF-α- and IL-1α-dependent pathways implied that conditions could be found in which EGFR and IL-1R signals were not perfectly balanced. At some concentrations, TGF-α might act as a prosurvival factor and at others as a proapoptotic factor. To test this idea, cells were exposed to TNF in combination with exogenous TGF-α at 0.3–100 ng/ml, and the fraction of dying cells was measured. We observed that, at low concentrations, TGF-α was proapoptotic in combination with TNF, whereas at higher concentrations, it was prosurvival (Figure 5J), confirming our prediction.

The link between the TGF-α and IL-1α autocrine circuits raised the possibility that additional extracellular factors might contribute to TNF signaling and cellular responses. In recent microarray studies, we observed that transcription of the *IL-1ra* gene was strongly upregulated by TNF (K.A.J. and P.K.S., unpublished data). ELISA measurements on conditioned medium of HT-29 cells revealed that IL-1ra protein accumulated to significant levels 12 hr after TNF stimulation (Figure 5K). However, unlike IL-1α, TNF-induced IL-1ra release was unaffected by pretreatment with C225 antibody, indicating that IL-1ra induction does not require autocrine TGF-α (Figure S5). Thus, IL-1ra constitutes a third TNF-inducible autocrine factor, one with a prosurvival function (Figure 5F; Dinarello, 2000).

The successive waves of extracellular signaling circuits induced by TNF suggest the existence of an autocrine cascade involving TNF, TGF-α, IL-1α, and IL-1ra. The most interesting features of the cascade are the connections between individual autocrine circuits: TGF-α is required for IL-1α release, and IL-1ra inhibits the action of IL-1α. Is there a contingent logic underlying the order in which these signals are released? We found that the link between TGF-α and IL-1α (Figure 5I) was not reciprocal because addition of exogenous IL-1α did not induce shedding of TGF-α (Figure 5L). Moreover, exogenous TGF-α was not sufficient to provoke IL-1α release (Figure 5M), implying that signals from both TNFR and EGFR are required. The TGF-α and IL-1α circuits are therefore linked together unidirectionally. TNF and TGF-α comprise inputs to an "AND" function that induces IL-1α, which is subsequently inactivated by IL-1ra (Figure 5N).

Evidence for a TNF-Induced Autocrine Cascade in Diverse Epithelial Cell Types

To examine whether TNF-induced autocrine cascades are a conserved feature of TNF-responsive cells, we tested other epithelial cell lines for the essential features of the TGF-α-IL-1α-IL-1ra cascade. Specifically, we asked whether TNF would stimulate (1) release of TGF-α (Figure 6A), (2) release of IL-1α in an EGFR-dependent manner (Figure 6B), and (3) release of IL-1ra (Figure 6C). We focused on two human cell lines known to have receptors for TNF, EGF, and IL-1: A431 epidermoid carcinoma cells and nontransformed 184A1 human mammary epithelial cells (HMEC; Chen et al., 2004; Masui et al., 1993).

Both A431 and immortalized HMEC cells were treated with TNF, and cytokine levels were measured at t = 0, 2, and 24 hr by ELISA (Figures 6D–6I). We found that TGF-α, IL-1α, and IL-1ra levels all increased in A431 cells after TNF treatment. In particular, TGF-α release was nearly as rapid as in HT-29 cells. TNF-stimulated IL-1α release in A431 cells was inhibited significantly but not completely by C225, probably reflecting incomplete blockade of high EGFR levels on the surface of these cells (Masui et al., 1993). In analogous experiments with TNF-simulated HMEC cells, we found that TGF-α levels increased dramatically over a 24 hr period, IL-1α levels increased >2.5-fold, and IL-1ra levels increased >4-fold. Moreover, TNF-induced release of IL-1α into the medium was blocked almost completely by C225 anti-EGFR antibody. Thus, all three extracellular components of the TNF-stimulated TGF-α-IL-1α-IL-1ra autocrine cascade are present in HMEC cells, and induction of the IL-1α circuit is almost completely dependent on prior establishment of the TGF-α-EGFR circuit. The primary difference between HT-29 and HMEC cells is in the timing of TGF-α release, which was considerably slower in HMECs, perhaps reflecting a requirement for protein synthesis. Together, these data indicate that a TNF-induced autocrine cascade consisting of TGF-α, IL-1α, and IL-1ra cytokines exists in multiple epithelial cell types.

DISCUSSION

In this paper, we show that TNF induces three successive autocrine circuits, which together form an autocrine cascade that plays out over 24 hr (Figure 7A). Working in combination with TNF itself, the cascade adds layers of pro- and antiapoptotic signaling to set the level of apoptosis in a self-limiting fashion. Shortly after TNF addition, proapoptotic signals immediately downstream of TNFR binding are induced. About 10 min later, an autocrine TGF-α circuit is established, leading to prosurvival signaling through EGFR. The combination of TNF and TGF-α causes release of IL-1α starting at 4 hr, which in turn activates prodeath signaling through IL-1R. Finally, upregulation of the IL-1R antagonist IL-1ra by 8–12 hr negatively regulates IL-1R signaling and presumably constitutes a final antiapoptotic stimulus. Our work highlights the important but underappreciated role of autocrine crosstalk in determining cell fate. Individual autocrine circuits have previously been studied in multiple cellular contexts. However, extended connectivity between inducible autocrine circuits has not been reported previously, perhaps because

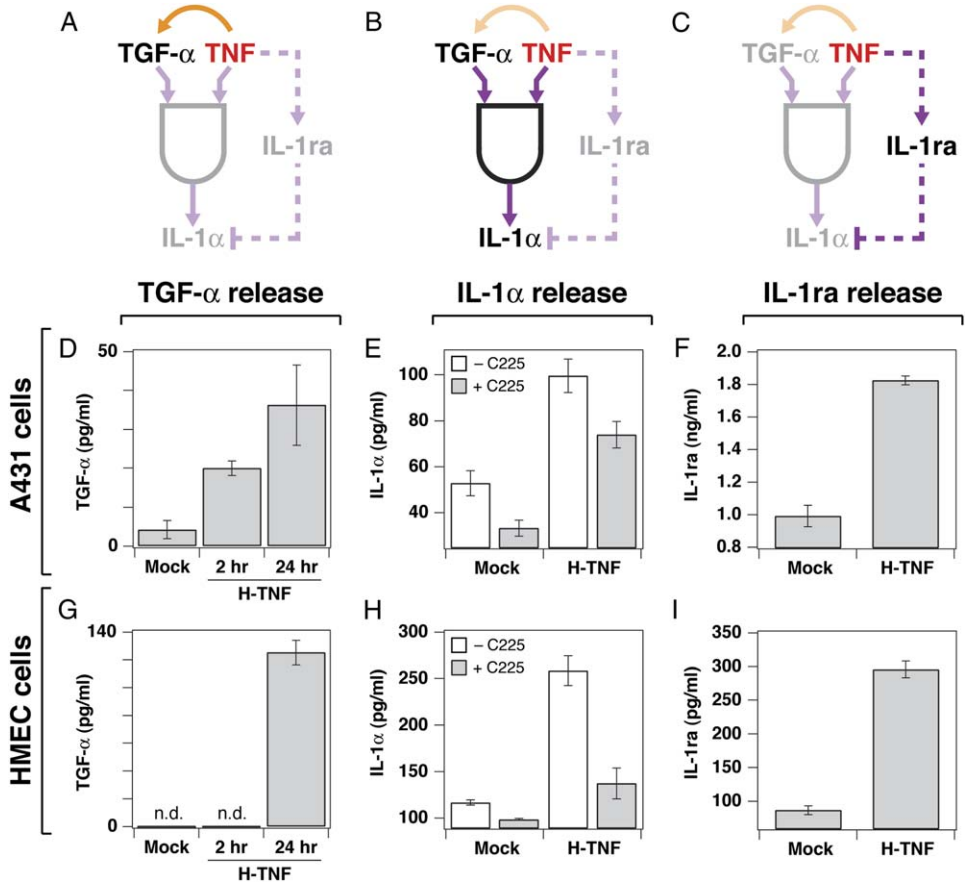

Figure 6. The Basic Elements of the TNF-Induced Autocrine Cascade Are Present in Other Epithelial Cell Types

(A–C) Main elements of the TNF-induced autocrine cascade: release of TGF-α (A), release of IL-1α in a TGF-α-dependent manner (B), and release of IL-1ra (C).

(D and E) The TNF-induced autocrine cascade exists in A431 cells. A431 cells were stimulated with 100 ng/ml TNF + 10 μg/ml C225 (H-TNF) (D–F) or 100 ng/ml TNF alone (E) and analyzed for TGF-α at 2 and 24 hr (D), IL-1α at 24 hr (E), and IL-1ra at 24 hr (F). The control treatment was a mock stimulation with carrier only.

(G–I) The TNF-induced autocrine cascade exists in human mammary epithelial cells (HMEC). HMEC cells were stimulated with 100 ng/ml TNF (H-TNF) (G–I) or 100 ng/ml TNF (H-TNF) + 10 μg/ml C225 (H) and analyzed for TGF-α at 2 and 24 hr (G), IL-1α at 24 hr (H), and IL-1ra at 24 hr (I). The control treatment was a mock stimulation with carrier only.

For (D)–(I), data are presented as the mean ± SEM of triplicate biological samples as described in Experimental Procedures. n.d., not detectable.

such linkages are only evident when large, multidimensional signaling data sets are examined.

Data, Statistical Mining, and Hypotheses

The construction of a systematic time-dependent compendium of cellular signals has been essential to our analysis of TNF. The 7980-measurement compendium contains quantitative information on 19 activities and states of kinases, caspases, transcription factors, adaptors, and other signaling proteins distributed across signaling networks downstream of TNFR, EGFR, and insulin receptor (Figure 1A). An advantage of constraining measurements to a limited number of proteins is that it becomes practical to examine many different cytokine combinations at multiple points in time. The experimental precision and reproducibility of the measurements also made it possible to study small (i.e., less than 2-fold) but biologically significant differences in signals from one cytokine treatment to the next. Our proteomic compendium is far from comprehensive, but, in the context of signal transduction, the multicomponent, multicytokine time courses represent a useful advance over more focused studies because they place dynamic information within a broader physiological context.

A major challenge with large experimental compendia is generating experimentally testable biological hypotheses. Here, we use DPLSR to derive a visually intuitive map from time-integrated signals (Janes et al., 2004). In related work, we construct alternative models that explicitly incorporate time-course data (Janes et al., 2005). Both analyses show that a TNF-induced autocrine cascade is critical in determining cell fate. However, it is important to note

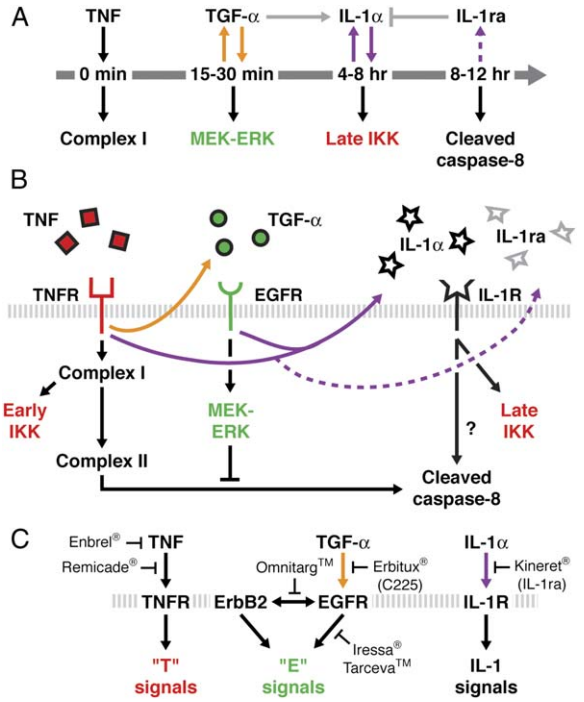

Figure 7. Model of TNF-Induced Extracellular Crosstalk

(A) Sequence of the time-dependent TNF-induced autocrine cascade established by TGF-α, IL-1α, and IL-1ra.

(B) Direct and autocrine-indirect intracellular signals activated by TNF.

(C) Approved pharmaceuticals that target different points of the TNF-induced autocrine cascade.

that, despite the importance of compendium data for hypothesis generation, critical features of the TNF-induced autocrine cascade were confirmed by independent experimentation without reference to DPLSR analysis. Hypothesis-testing experiments took advantage of highly specific (and clinically important) inhibitors of EGF and IL-1 signaling.

Intracellular Regulators of the TNF-Induced Autocrine Cascade

This study focuses on the role played by extracellular crosstalk in the response of cells to TNF (Figure 7B). However, intracellular crosstalk is equally important for regulating signaling proteins by two or more receptor types. We estimate that ~50% of signaling in HT-29 cells is attributable to autocrine factors induced by TNF and ~50% is dependent on direct signals downstream of TNFR. One clear point of intersection between internal and external signals is the regulation of metalloproteases and calpains, which cleave inactive membrane bound precursors to promote TGF-α and IL-1α shedding (Kobayashi et al., 1990; Peschon et al., 1998). The importance of metalloprotease and calpain activity for the TNF autocrine cascade is demonstrated by the effectiveness of small-molecule protease inhibitors in blocking autocrine ligand release. Regulation of membrane proteases is an area of active research (Goll et al., 2003), and increasing evidence suggests a role for protease phosphorylation (Fan and Derynck, 1999; Glading et al., 2004). However, current understanding of metalloprotease and calpain phosphorylation is insufficient to explain the dynamics of the TNF-induced autocrine cascade in HT-29 cells. For example, ERK has been implicated in cytokine-stimulated shedding of TGF-α (Fan and Derynck, 1999). However, most TNF-induced ERK activation occurs as a consequence (rather than a cause) of TGF-α release. Detailed analysis of protease regulation will be critical to understanding the autocrine cascades described here.

Molecular Logic of the Autocrine Cascade

TNF is known to stimulate the release of many soluble factors, but most are thought to act in a paracrine fashion (Pahl, 1999); very few studies have established a role for TNF in autocrine signaling (Chen et al., 2004). Likewise, crosstalk in intracellular networks is well recognized (Dumont et al., 2002), but extracellular crosstalk involving multiple autocrine signals has not been explicitly documented. The most striking feature of the TNF-induced autocrine cascade described here is its conditional "molecular logic." Activation of the IL-1α circuit requires prior TGF-α release, but TGF-α-IL-1α interaction depends on the presence of TNF because exogenous TGF-α alone does not cause IL-1α release. TGF-α-IL-1α crosstalk is also unidirectional: exogenous IL-1α does not cause TGF-α release. Likewise, IL-1ra is presumed to inhibit IL-1α signaling (Dinarello, 2000), but IL-1ra release is almost completely TNF dependent: it is only slightly decreased by EGFR blockade and only slightly induced by exogenous IL-1α (K.A.J. and P.K.S., unpublished data). These and other data reemphasize the complexity and current lack of understanding of the metalloprotease and calpain regulation in autocrine signaling.

Biological and Clinical Significance

Why does the response of cells to TNF involve complex self-limiting extracellular signals? Overlapping positive and negative feedback has been proposed as a means to optimize the sensitivity and stability of biological systems (Stelling et al., 2004). A role for autocrine circuits in sensing spatial ranges and local environmental cues has also been documented (Wiley et al., 2003). In agreement with this, we have found that the precise magnitude of autocrine-dependent apoptotic responses is cell-density dependent (J.G.A. and P.K.S., unpublished data). Our data suggest that TNF-induced cytokines do not travel far before rebinding to cells, but we have not yet established whether they bind to the original secreting cell in true-autocrine mode or whether they diffuse to adjacent cells in a paracrine fashion. Regardless, it seems likely that the TNF-TGF-α-IL-1α-IL-1ra cascade functions to link cell-death decisions to extracellular cues and thereby achieve microenvironment-sensitive control over cell fate (Figure 7A).

In the current work, we rely entirely on immortalized cells grown in vitro. It will now be important to study TNF-induced autocrine cascades in primary cells, such as hepatocytes and adipocytes, in which TNF has established physiological and pathological roles (Ruan and Lodish, 2003; Streetz et al., 2000). However, the TNF-induced autocrine cascade discovered in HT-29 cells clearly operates in a variety of other transformed and nontransformed cell lines. Like HT-29 cells, A431 and HMEC cells have inducible TNF-TGF-α-IL-1α-IL-1ra circuits, although the timing and magnitude of each loop in the cascade appears to vary. This suggests that the extent of crosstalk between autocrine and intracellular networks, and their relative physiological importance, may depend on cell type and stimulus. The cell-type specificity of the TNF-induced autocrine cascade clearly warrants further investigation.

Since its discovery three decades ago as an endotoxin-induced serum factor with tumoricidal activity, TNF has remained an important therapeutic target in a variety of human diseases (Carswell et al., 1975; Palladino et al., 2003). Neutralizing anti-TNF antibodies (e.g., Remicade) and decoy receptors (e.g., Enbrel) are now used to treat inflammatory bowel disease and rheumatoid arthritis (Figure 7C; Rutgeerts et al., 2004; Sfikakis and Kollias, 2003). However, clinical trials on sepsis and cancer, once promising targets for TNF treatment, have been disappointing and have highlighted the puzzling inefficacy and side effects of cytokine-directed therapy (Anderson et al., 2004; Reinhart and Karzai, 2001). Our experiments provide some insight into why therapeutics targeted against self-limiting autocrine systems are so difficult to design. For example, the treatment of TNF-stimulated HT-29 cells with the anti-EGFR antibody C225 (known commercially as Erbitux) does not increase the level of apoptosis, even though it causes extensive changes in both intracellular and extracellular signaling. It is not that Erbitux is inactive against HT-29 cells, but rather that proapoptotic effects of blocking TGF-α are offset by a reduction in IL-1α levels. Understanding how autocrine cascades operate in normal and diseased tissues seems likely to yield significant therapeutic insight, particularly with respect to multidrug therapies. Indeed, combination treatments involving anti-TNF biologics and IL-1ra are already being explored for the treatment of rheumatoid arthritis (Zwerina et al., 2004).

EXPERIMENTAL PROCEDURES

Cell-Line Treatments and Lysis

HT-29 cells were grown, plated, and sensitized with IFN-γ as described previously (Janes et al., 2003). Sensitized cells were then spiked with 0, 0.2, 5, 100 ng/ml TNF (Peprotech) + 0, 1, 100 ng/ml EGF (Peprotech) or 0, 1, 5, 500 ng/ml insulin (Sigma) as a 20× stock in serum-free medium. Triplicate plates were lysed at the indicated times as described (Gaudet et al., 2005; Janes et al., 2003). For TGF-α perturbation, C225, batimastat (both gifts from H.S. Wiley), AG1478 (Calbiochem), and anti-TGF-α antibody (R&D Systems) were added 1 hr before stimulation. For IL-1α perturbation, IL-1ra (R&D Systems), ALLM, PD150606 (both from Calbiochem), and anti-IL-1α antibody (R&D Systems) were added at the same time as stimulation. A431 cells (ATCC) and the HMEC line (Stampfer and Yaswen, 1993) were maintained in recommended growth medium, plated at 20,000 cells/cm^2, and sensitized and treated as described for HT-29 cells.

Network-Level Signaling Measurements

Kinase assays, Western blotting, and antibody microarrays were essentially performed as described (Janes et al., 2003, 2004; Nielsen et al., 2003). The full quantitative details of the network-level signaling measurements are reported elsewhere (Gaudet et al., 2005). The final processed data were normalized to the maximum value (across all conditions) for that signal to aid comparison of signals with different dynamic ranges.

DPLSR Mapping

Nine of ten cytokine treatments (all except 0.2 ng/ml TNF + 1 ng/ml insulin) were used for the DPLSR mapping. The signaling network dynamics were integrated by trapezoidal rule to calculate a composite metric for each signal within each time course. The integrated signals and treatment classes were mapped by DPLSR as described previously (Janes et al., 2004) and in Figure S1.

Enzyme-Linked Immunosorbent Assays

Conditioned medium from HT-29, A431, and HMEC cultures was analyzed for TGF-α, AR, HB-EGF, IL-1α, IL-1β, and IL-1ra according to manufacturer's recommendations (R&D Systems).

Indirect Immunofluorescence

Cells were fixed with 4% paraformaldehyde in PBS for 10 min at room temperature, then permeabilized with Perm/Wash (BD Biosciences) and stained with anti-RelA (Santa Cruz, 1:100) and Alexa 594 anti-rabbit IgG (Molecular Probes, 1:250). Coverslips were mounted with VectaShield, and imaging was performed with a 63× Plan-Apochromat objective and a Photometrics CoolSnap HQ camera on a DeltaVision RT Restoration microscope. 0.2 μm Z sections were acquired and deconvolved using Applied Precision SoftWorx software. Images are shown as individual slices from the reconstructed 3D image.

Apoptosis Measurements

Cells that scored double positive for cleaved cytokeratin (a caspase-3/6/7 substrate) and cleaved-caspase-3 were measured by flow cytometry or by annexin V-propidium iodide staining as described previously (Janes et al., 2003). Changes in survival were calculated as before (Janes et al., 2003).

Statistical Analysis

Covariations within the TNF-EGF-insulin network were calculated as the Euclidean distance between the signals and the cytokine cues on the DPLSR mapping (Figure 2); a Bonferroni-corrected Student's paired t test was used to compare Euclidean distances. For comparing two individual means, a Student's t test was used. For comparing two time courses, a two-way analysis of variance was used. All tests were performed at a significance level of $\alpha = 0.05$ with Bonferroni correction for multiple hypothesis testing when appropriate.

Supplemental Data

Supplemental Data include Supplemental References, five figures, and three tables and can be found with this article online at http://www.cell.com/cgi/content/full/124/6/1225/DC1/.

ACKNOWLEDGMENTS

We thank Michael Yaffe (MIT) and Steve Wiley (PNNL) for providing critical reagents and for helpful discussions, Emily Pace (Merrimack) for technical assistance with the antibody microarrays, and members of the Sorger and Lauffenburger laboratory who helped with experiments. This work was supported by NIH grant P50-GM68762 (P.K.S. and D.A.L.) and the Whitaker Foundation (K.A.J.). P.K.S. is a founder and chair of the Scientific Advisory Board of Merrimack

Pharmaceuticals. D.A.L. is a member of the Scientific Advisory Board of Merrimack Pharmaceuticals.

Received: May 26, 2005
Revised: October 19, 2005
Accepted: January 5, 2006
Published: March 23, 2006

REFERENCES

Aggarwal, B.B. (2003). Signalling pathways of the TNF superfamily: a double-edged sword. Nat. Rev. Immunol. *3*, 745–756.

Anderson, G.M., Nakada, M.T., and DeWitte, M. (2004). Tumor necrosis factor-alpha in the pathogenesis and treatment of cancer. Curr. Opin. Pharmacol. *4*, 314–320.

Anzano, M.A., Rieman, D., Prichett, W., Bowen-Pope, D.F., and Greig, R. (1989). Growth factor production by human colon carcinoma cell lines. Cancer Res. *49*, 2898–2904.

Avruch, J. (1998). Insulin signal transduction through protein kinase cascades. Mol. Cell. Biochem. *182*, 31–48.

Ballif, B.A., and Blenis, J. (2001). Molecular mechanisms mediating mammalian mitogen-activated protein kinase (MAPK) kinase (MEK)-MAPK cell survival signals. Cell Growth Differ. *12*, 397–408.

Barnhart, B.C., and Peter, M.E. (2003). The TNF receptor 1: a split personality complex. Cell *114*, 148–150.

Bender, K., Gottlicher, M., Whiteside, S., Rahmsdorf, H.J., and Herrlich, P. (1998). Sequential DNA damage-independent and -dependent activation of NF-kappaB by UV. EMBO J. *17*, 5170–5181.

Carswell, E.A., Old, L.J., Kassel, R.L., Green, S., Fiore, N., and Williamson, B. (1975). An endotoxin-induced serum factor that causes necrosis of tumors. Proc. Natl. Acad. Sci. USA *72*, 3666–3670.

Chailler, P., and Menard, D. (1999). Ontogeny of EGF receptors in the human gut. Front. Biosci. *4*, D87–D101.

Chen, G., and Goeddel, D.V. (2002). TNF-R1 signaling: a beautiful pathway. Science *296*, 1634–1635.

Chen, W.N., Woodbury, R.L., Kathmann, L.E., Opresko, L.K., Zangar, R.C., Wiley, H.S., and Thrall, B.D. (2004). Induced autocrine signaling through the epidermal growth factor receptor contributes to the response of mammary epithelial cells to tumor necrosis factor alpha. J. Biol. Chem. *279*, 18488–18496.

Dinarello, C.A. (1997). Interleukin-1. Cytokine Growth Factor Rev. *8*, 253–265.

Dinarello, C.A. (2000). The role of the interleukin-1-receptor antagonist in blocking inflammation mediated by interleukin-1. N. Engl. J. Med. *343*, 732–734.

Downward, J. (2001). The ins and outs of signalling. Nature *411*, 759–762.

Dumont, J.E., Dremier, S., Pirson, I., and Maenhaut, C. (2002). Cross signaling, cell specificity, and physiology. Am. J. Physiol. Cell Physiol. *283*, C2–C28.

Efron, B., and Tibshirani, R.J. (1993). An Introduction to the Bootstrap (London: Chapman and Hall).

Fan, H., and Derynck, R. (1999). Ectodomain shedding of TGF-alpha and other transmembrane proteins is induced by receptor tyrosine kinase activation and MAP kinase signaling cascades. EMBO J. *18*, 6962–6972.

Fransen, L., Van der Heyden, J., Ruysschaert, R., and Fiers, W. (1986). Recombinant tumor necrosis factor: its effect and its synergism with interferon-gamma on a variety of normal and transformed human cell lines. Eur. J. Cancer Clin. Oncol. *22*, 419–426.

Garcia-Lloret, M.I., Yui, J., Winkler-Lowen, B., and Guilbert, L.J. (1996). Epidermal growth factor inhibits cytokine-induced apoptosis of primary human trophoblasts. J. Cell. Physiol. *167*, 324–332.

Gaudet, S., Janes, K.A., Albeck, J.G., Pace, E.A., Lauffenburger, D.A., and Sorger, P.K. (2005). A compendium of signals and responses triggered by prodeath and prosurvival cytokines. Mol. Cell. Proteomics *4*, 1569–1590.

Glading, A., Bodnar, R.J., Reynolds, I.J., Shiraha, H., Satish, L., Potter, D.A., Blair, H.C., and Wells, A. (2004). Epidermal growth factor activates m-calpain (calpain II), at least in part, by extracellular signal-regulated kinase-mediated phosphorylation. Mol. Cell. Biol. *24*, 2499–2512.

Goll, D.E., Thompson, V.F., Li, H., Wei, W., and Cong, J. (2003). The calpain system. Physiol. Rev. *83*, 731–801.

Hambek, M., Solbach, C., Schnuerch, H.G., Roller, M., Stegmueller, M., Sterner-Kock, A., Kiefer, J., and Knecht, R. (2001). Tumor necrosis factor alpha sensitizes low epidermal growth factor receptor (EGFR)-expressing carcinomas for anti-EGFR therapy. Cancer Res. *61*, 1045–1049.

Hofmann, F., and Garcia-Echeverria, C. (2005). Blocking the insulin-like growth factor-I receptor as a strategy for targeting cancer. Drug Discov. Today *10*, 1041–1047.

Izumi, H., Ono, M., Ushiro, S., Kohno, K., Kung, H.F., and Kuwano, M. (1994). Cross talk of tumor necrosis factor-alpha and epidermal growth factor in human microvascular endothelial cells. Exp. Cell Res. *214*, 654–662.

Janes, K.A., Albeck, J.G., Peng, L.X., Sorger, P.K., Lauffenburger, D.A., and Yaffe, M.B. (2003). A high-throughput quantitative multiplex kinase assay for monitoring information flow in signaling networks: application to sepsis-apoptosis. Mol. Cell. Proteomics *2*, 463–473.

Janes, K.A., Kelly, J.R., Gaudet, S., Albeck, J.G., Sorger, P.K., and Lauffenburger, D.A. (2004). Cue-signal-response analysis of TNF-induced apoptosis by partial least squares regression of dynamic multivariate data. J. Comput. Biol. *11*, 544–561.

Janes, K.A., Albeck, J.G., Gaudet, S., Sorger, P.K., Lauffenburger, D.A., and Yaffe, M.B. (2005). A predictive systems model of signaling identifies a molecular basis set for cytokine-induced apoptosis. Science *310*, 1646–1653.

Karin, M., and Ben-Neriah, Y. (2000). Phosphorylation meets ubiquitination: the control of NF-[kappa]B activity. Annu. Rev. Immunol. *18*, 621–663.

Karin, M., and Greten, F.R. (2005). NF-kappaB: linking inflammation and immunity to cancer development and progression. Nat. Rev. Immunol. *5*, 749–759.

Kobayashi, Y., Yamamoto, K., Saido, T., Kawasaki, H., Oppenheim, J.J., and Matsushima, K. (1990). Identification of calcium-activated neutral protease as a processing enzyme of human interleukin 1 alpha. Proc. Natl. Acad. Sci. USA *87*, 5548–5552.

Masui, H., Castro, L., and Mendelsohn, J. (1993). Consumption of EGF by A431 cells: evidence for receptor recycling. J. Cell Biol. *120*, 85–93.

Mendelsohn, J., and Baselga, J. (2000). The EGF receptor family as targets for cancer therapy. Oncogene *19*, 6550–6565.

Micheau, O., and Tschopp, J. (2003). Induction of TNF receptor I-mediated apoptosis via two sequential signaling complexes. Cell *114*, 181–190.

Micheau, O., Lens, S., Gaide, O., Alevizopoulos, K., and Tschopp, J. (2001). NF-kappaB signals induce the expression of c-FLIP. Mol. Cell. Biol. *21*, 5299–5305.

Micheau, O., Thome, M., Schneider, P., Holler, N., Tschopp, J., Nicholson, D.W., Briand, C., and Grutter, M.G. (2002). The long form of FLIP is an activator of caspase-8 at the Fas death-inducing signaling complex. J. Biol. Chem. *277*, 45162–45171.

Nicholson, D.W., and Thornberry, N.A. (1997). Caspases: killer proteases. Trends Biochem. Sci. *22*, 299–306.

Nielsen, U.B., Cardone, M.H., Sinskey, A.J., MacBeath, G., and Sorger, P.K. (2003). Profiling receptor tyrosine kinase activation by using Ab microarrays. Proc. Natl. Acad. Sci. USA *100*, 9330–9335.

Pahl, H.L. (1999). Activators and target genes of Rel/NF-kappaB transcription factors. Oncogene *18*, 6853–6866.

Palladino, M.A., Bahjat, F.R., Theodorakis, E.A., and Moldawer, L.L. (2003). Anti-TNF-alpha therapies: the next generation. Nat. Rev. Drug Discov. *2*, 736–746.

Panja, A., Goldberg, S., Eckmann, L., Krishen, P., and Mayer, L. (1998). The regulation and functional consequence of proinflammatory cytokine binding on human intestinal epithelial cells. J. Immunol. *161*, 3675–3684.

Peschon, J.J., Slack, J.L., Reddy, P., Stocking, K.L., Sunnarborg, S.W., Lee, D.C., Russell, W.E., Castner, B.J., Johnson, R.S., Fitzner, J.N., et al. (1998). An essential role for ectodomain shedding in mammalian development. Science *282*, 1281–1284.

Qian, H., Hausman, D.B., Compton, M.M., Martin, R.J., Della-Fera, M.A., Hartzell, D.L., and Baile, C.A. (2001). TNFalpha induces and insulin inhibits caspase 3-dependent adipocyte apoptosis. Biochem. Biophys. Res. Commun. *284*, 1176–1183.

Reinhart, K., and Karzai, W. (2001). Anti-tumor necrosis factor therapy in sepsis: update on clinical trials and lessons learned. Crit. Care Med. *29*, S121–S125.

Ruan, H., and Lodish, H.F. (2003). Insulin resistance in adipose tissue: direct and indirect effects of tumor necrosis factor-alpha. Cytokine Growth Factor Rev. *14*, 447–455.

Rutgeerts, P., Van Assche, G., and Vermeire, S. (2004). Optimizing anti-TNF treatment in inflammatory bowel disease. Gastroenterology *126*, 1593–1610.

Schlessinger, J. (2004). Common and distinct elements in cellular signaling via EGF and FGF receptors. Science *306*, 1506–1507.

Schulze, A., Lehmann, K., Jefferies, H.B., McMahon, M., and Downward, J. (2001). Analysis of the transcriptional program induced by Raf in epithelial cells. Genes Dev. *15*, 981–994.

Sfikakis, P.P., and Kollias, G. (2003). Tumor necrosis factor biology in experimental and clinical arthritis. Curr. Opin. Rheumatol. *15*, 380–386.

Singh, P., and Rubin, N. (1993). Insulinlike growth factors and binding proteins in colon cancer. Gastroenterology *105*, 1218–1237.

Stampfer, M.R., and Yaswen, P. (1993). Culture systems for study of human mammary epithelial cell proliferation, differentiation and transformation. Cancer Surv. *18*, 7–34.

Stelling, J., Sauer, U., Szallasi, Z., Doyle, F.J., 3rd, and Doyle, J. (2004). Robustness of cellular functions. Cell *118*, 675–685.

Streetz, K., Leifeld, L., Grundmann, D., Ramakers, J., Eckert, K., Spengler, U., Brenner, D., Manns, M., and Trautwein, C. (2000). Tumor necrosis factor alpha in the pathogenesis of human and murine fulminant hepatic failure. Gastroenterology *119*, 446–460.

Torrance, C.J., Jackson, P.E., Montgomery, E., Kinzler, K.W., Vogelstein, B., Wissner, A., Nunes, M., Frost, P., and Discafani, C.M. (2000). Combinatorial chemoprevention of intestinal neoplasia. Nat. Med. *6*, 1024–1028.

Wajant, H., Pfizenmaier, K., and Scheurich, P. (2003). Tumor necrosis factor signaling. Cell Death Differ. *10*, 45–65.

Wiley, H.S., Shvartsman, S.Y., and Lauffenburger, D.A. (2003). Computational modeling of the EGF-receptor system: a paradigm for systems biology. Trends Cell Biol. *13*, 43–50.

Wu, Y., Tewari, M., Cui, S., and Rubin, R. (1996). Activation of the insulin-like growth factor-I receptor inhibits tumor necrosis factor-induced cell death. J. Cell. Physiol. *168*, 499–509.

Zwerina, J., Hayer, S., Tohidast-Akrad, M., Bergmeister, H., Redlich, K., Feige, U., Dunstan, C., Kollias, G., Steiner, G., Smolen, J., and Schett, G. (2004). Single and combined inhibition of tumor necrosis factor, interleukin-1, and RANKL pathways in tumor necrosis factor-induced arthritis: effects on synovial inflammation, bone erosion, and cartilage destruction. Arthritis Rheum. *50*, 277–290.